Genetic ablation of bone marrow beta-adrenergic receptors in mice modulates miRNA-transcriptome networks of neuroinflammation in the paraventricular nucleus

Christopher J. Martyniuk[1]*, Ruben Martinéz[2,3], Daniel J. Kostyniuk[4], Jan A. Mennigen[4], and Jasenka Zubcevic[1*]

[1]Department of Physiological Sciences, College of Veterinary Medicine, University of Florida, Gainesville, FL 32610

[2]Department of Environmental Chemistry, Institute of Environmental Assessment and Water Research, IDAEA-CSIC, Jordi Girona, Barcelona 18-26 08034, Spain.

[3]Department of Cellular Biology, Physiology and Immunology, Universidad de Barcelona (UB), Barcelona 585 08007, Spain.

[4]Department of Biology, University of Ottawa, Ottawa, Ontario K1N 6N5, Canada.

Running Head: Molecular responses in the PVN with bone marrow ablation

***Corresponding authors contact information:**

Department of Physiological Sciences, College of Veterinary Medicine, University of Florida PO BOX 100274 GAINESVILLE FL 326100274 United States; Email: jasenkaz@ufl.edu and cmartyn@ufl.edu

Total words:

Abstract. Elucidating molecular pathways regulating neuroimmune communication is critical for therapeutic interventions in conditions characterized by overactive immune responses and dysfunctional autonomic nervous system. We generated a bone marrow-specific adrenergic beta 1 and beta 2 knockout mouse chimera (AdrB1.B2 KO) to determine how sympathetic drive to the bone affects transcripts and miRNAs in the hypothalamic paraventricular nucleus (PVN). This model has previously exhibited a dampened systemic immune response and decreased blood pressure compared to control animals. Reduced sympathetic responsiveness of the bone marrow hematopoietic cells of AdrB1.B2 KO chimera led to suppression of transcriptional networks that included leukocyte cell adhesion and migration and T cell-activation and recruitment. Transcriptome responses related to IL-17a signaling and the renin-angiotensin system (RAS) were also suppressed in the PVN. Based on the transcriptome response, we next computationally predicted miRNAs in the PVN that may underscore the reduced sympathetic responsiveness of the bone marrow cells. These included miR-27b-3p, miR-150, miR-223-3p, and miR-326. Using real-time PCR, we measured a downregulation in the expression of miR-150-5p, miR-205-5p, miR-223-3p, miR-375-5p, miR-499a-5p, miR-27b-3p, let-7a-5p, and miR-21a-5p in the PVN of AdrB1.B2 KO chimera, confirming computational predictions that these miRNAs are associated with reduced neuro-immune responses and the loss of sympathetic responsiveness in the bone marrow. Intriguingly, directional responses of the miRNA corresponded to mRNAs, suggesting complex temporal or circuit-dependent posttranscriptional control of gene expression in the PVN. This study identifies molecular pathways involved in neural-immune interactions that may act as targets of therapeutic intervention for a dysfunctional autonomic nervous system.

Key words: neuro-immune, transcriptomics, network analysis, sympathetic nervous system, bone marrow

Introduction

Many conditions are marked by autonomic nervous system dysfunction and aberrant immune responses, including cardiovascular, metabolic and neurological

conditions (2, 12, 44). The central nervous system (CNS) is a primary control center of neuro-immune communication, as generation of the sympathetic input within brain regions such as the periventricular nucleus (PVN) affects visceral and peripheral immune tissues including the bone marrow. During homeostasis, immune cell proliferation, maturation, and release from the bone are in part regulated by the sympathetic nervous system via adrenergic beta 1 and beta 2 receptors (21, 22, 29). An increase in the sympathetic drive in conditions like hypertension and heart failure contributes to exaggerated bone marrow-associated immune responses and consequent infiltration of activated immune cells into tissues including the brain (3, 18), which can lead to neuroinflammatory responses that negatively impact neuronal function.

Our previous studies described a chimera bone marrow model that is characterized by a reduced effect of the sympathetic drive to the bone hematopoietic cells (4, 40). As a consequence of this, the chimera mice show suppressed expression of immune gene networks in the bone marrow, reduced circulating levels of inflammatory T cells, macrophages and neutrophils, and lower blood pressure at night when the mice are most active (4). In addition, these mice present with a marked reduction in tissue-infiltrating inflammatory cells and suppression in immune transcriptome networks in the host gastrointestinal (GI) system, which is also associated with a shift in the gut bacterial richness towards more beneficial microbiota (40). Taken together, these data suggest that dampening of the sympatho-immune interaction in the bone marrow leads to immunosuppression that can in turn affect the cardiovascular and GI function. Conversely, sympatho-activation of the bone marrow immune responses resulted in infiltration of the immune cells into the PVN, which was associated with neuroinflammation and further increase in the sympathetic drive in a rodent model of hypertension (3). Thus, both peripheral and central neuro-immune interaction are critical in maintaining physiological homeostasis of the sympathetic and autonomic nervous system. However, the molecular mechanisms underlying neuro-immune communication in the brain, i.e. the glial-neural communication as opposed to sympatho-immune communication in the bone, are not fully elucidated.

The main objective of this study was to characterize the molecular networks in the PVN of mice that have been treated with bone marrow ablation and reconstitution approaches leading to reduced sympathetic responsiveness of the bone marrow hematopoietic cells. This novel model allows us to isolate the effects of bone marrow-derived immune cells on the PVN. Based upon our previous transcriptome studies in the bone and gastrointestinal system of this model (4, 40), and our previous studies showing neuroinflammatory effects of infiltrating activated bone marrow immune cells in hypertensive rat models (3, 31), we hypothesized that reduction in bone marrow sympathetic responsiveness would suppress immune-associated transcriptome networks in the PVN. In addition, we evaluated specific microRNAs that may regulate the changing transcriptome in the PVN as data suggest that miRNAs are important in the etiology of neuroinflammatory processes (14, 35). We used a two-tiered approach and first leveraged a computational approach to predict miRNA regulators of the transcriptome response in the PVN and subsequently quantified expression of candidate miRNAs using real-time PCR. These molecular data may shed light into central neural responses associated with reduced sympathetic responsiveness of the bone marrow cells.

2. Methods

2.1 Animal models

All experimental procedures were approved by the University of Florida Institute of Animal Care and Use Committee and complied with the standards stated in the National Institutes of Health Guide for the Care and Use of Laboratory Animals. Male mice (from 6 weeks old) were housed separately, in a temperature-controlled room (22°C to 23°C) with a 12:12-hour light-dark cycle, in specific-pathogen free cages, and had access to standard chow and water *ad libitum*.

2.2 Generating beta 1 and 2 adrenergic receptor knock out (KO) BM chimera mice

We utilized a novel BM chimera mouse model in order to specifically and solely block the effects of sympathetic nervous system on bone marrow immune cells, and subsequently investigate molecular mechanisms of immune-neural interaction in the PVN. Eight-week

old male AdrB1^{tm1Bkk}AdrB2^{tm1Bkk}/J, stock number 003810, were purchased from the Jackson Laboratory. These mice are homozygous null for the adrenergic receptor beta 1 (Adrb1) and beta 2 (Adrb2) genes, are viable, fertile, normal in size, and do not display any gross physical or behavioral abnormalities. Furthermore, these mice have no reported differences in hematopoiesis compared to normal mice (4). Mice were euthanized, and the whole bone marrow was extracted using established methods (4, 40). Whole bone marrow cells from AdrB1^{tm1Bkk}AdrB2^{tm1Bkk}/J mice were reconstituted to near lethally-irradiated (X ray, 950 Rad) six weeks old male C57BL/6J mice using a single retro-orbital injection at a ratio of 1:4 (donor:recipient), to generate the bone marrow AdrB1.B2 KO chimera mice. Control chimera mice (C57 chimera) were generated by reconstitution of C57BL/6J whole bone marrow cells into sub lethally-irradiated age- and sex-matched C57BL/6J mice using comparable irradiation and reconstitution protocols. The success of bone marrow ablation and reconstitution was confirmed by real time PCR in the circulating mononuclear cells (MNCs) using Taq Man primers for the Adrb1 and Adrb2 receptors (ThermoFisher Scientific catalogue#4331182) as before (4). All reconstituted mice were allowed to recover for 3 months prior to brain tissue collections.

2.3 RNA extraction from PVN of mice for microarray analysis

All mice were euthanized using isoflurane prior to whole brain extraction. Mouse brain slicer matrix (Zivic Instruments, PA, USA) was used to extract one coronal slice per mouse that encompassed 1mm of tissue with borders of the pituitary stalk as a rostro-caudal landmark. The PVN was punched out in each mouse at the 3rd ventricle and combined bilaterally for RNA extraction. Extraction of RNA from the PVN was performed using 1 mL TRIzol® Reagent (Life Technologies, Carlsbad, CA) as per manufacturer's protocol and our previous methods (4). Final nucleic acid pellets were resuspended in 30 µL RNAse-DNAse free water. Total RNA integrity for all samples used in microarray and real-time PCR analyses was determined using the RNA 6000 Nano Assay Kit with the 2100 Bioanalyzer (Agilent Technologies, Santa Clara, CA). The mean RNA integrity value for all samples used in the study was 9.41 (SEM ± 0.11).

2.4 Mouse PVN microarray analysis and bioinformatics

The SurePrint G3 Mouse GE 8x60K Microarray Kit (Agilent Product Number, G4852A Design ID 028005) was used to determine differentially expressed transcripts (n=8 per group). Briefly, RNA was purified using the RNeasy Mini Kit as per manufacture's protocol (Qiagen, Valencia, CA, USA). Microarray hybridizations were performed using high quality RNA (RIN>8) according to the One-Color Microarray-Based Gene Expression Analysis Low Input Quick Amp Labeling kit (Agilent V6.5, May 2010). Approximately 50 ng total RNA per sample was labelled and hybridized as per our previous publications (40). Microarrays were scanned at 5 μM with the Agilent G2505C Microarray Scanner. Raw signal intensities were extracted using the Agilent Feature Extraction Software (v. 10.1.1.1). All arrays were deemed high quality following manual inspection and quality control. Raw microarray data have been deposited into the NCBI Gene Expression Omnibus (GEO) database (Series GSE71633, GPL13912 Agilent-028005 SurePrint G3 Mouse GE 8x60K Microarray). Raw intensity data were imported into JMP® Genomics v7.0 (SAS Institute Inc., Cary, NC, USA). Intensity data were normalized using quantile normalization. Control probes were filtered out prior to identifying differentially expressed genes (DEGs) and the limit of detection was set to an intensity of 2.2 based on the Agilent spike in controls. Any probe falling below this value was assigned a normalized intensity of 2.2. DEGs were identified using a one-way analysis of variance (ANOVA) followed by a false discovery rate (FDR) set at 5.0%.

Cluster analysis was conducted in JMP Genomics v7.0 using all gene data. Two-way clustering using the Fast ward algorithm was conducted after each row was centered to a mean of zero (0) and variance scaled to one. Pathway Studio 9.0 (Elsevier) and ResNet 10.0 were utilized for sub-network enrichment analysis (SNEA) as per Ahmari and colleagues (4). The option of "best p-value, highest magnitude fold change" was selected for handling multiple probes of the same gene. There were 32,734 mouse probes successfully mapped using the official gene name in Pathway Studio. The SNEA was used to determine which gene networks were perturbed in the PVN. A Kolmogorov–Smirnov test with 500 permutations was conducted to determine whether certain networks were preferentially regulated compared to the background reference probability distribution. The enrichment P-value for a gene seed was set at $P < 0.05$. Lastly, we

conducted an *in silico* analysis in Pathway Studio (default settings) by querying, what the predicted posttranscriptional miR regulators for the observed transcriptional response were.

2.5 Real-time PCR validation of mouse transcripts

For mouse microarray validation, primer sets from target genes were collected from primerbank **(Supplemental Table T1) (**https://figshare.com/s/072e26dcb265d4d48d63, 10.6084/m9.figshare.11495076**)** (38). Transcripts that showed significant changes in expression levels were selected for microarray validation. The genes investigated included Tnnt1 (Troponin T1, Slow Skeletal Type) and Prkcd (Protein Kinase C Delta) due to their high fold change in the PVN following bone marrow reconstitutions (N=7-8/group). PCR was performed on CFX96 Touch™ Real-Time PCR Detection System (Bio-Rad, Hercules, California). The PCR conditions were as follows: 95 °C for 3 min, followed by 40 cycles of 95 °C for 30s, primer annealing at 60 °C for 30s, and 72 °C for 30s. Dissociation curves were generated, starting at 65 °C and ending at 95 °C with increments of 0.5 °C every 5 s. Gene expression was normalized to Gapdh and was determined using the relative ΔΔCt method (19) based on the method described. No reverse transcriptase control was used to assess presence of genomic DNA contamination.

2.6 miRNA quantification

Total RNA obtained from the previously described TRIzol® Reagent procedure was used to synthesize cDNA with HiFlex buffer using the miScript II RT kit (Qiagen, Toronto, ON, Canada) according to the manufacturer's instructions. Specific miRNAs were subsequently quantified using the miScript SYBR Green PCR kit (Qiagen) with miRNA-specific forward primers and a universal reverse primer **(Supplemental Table T2 (**https://figshare.com/s/072e26dcb265d4d48d63, 10.6084/m9.figshare.11495076**).** A standard curve consisting of serial dilutions of pooled cDNA, as well as a negative no-RT control consisting of cDNA generated in a reaction that did not include reverse transcriptase was run in duplicate. Reactions were run on a CFX96 instrument (Bio-Rad)

with a total volume of 25 µl containing 2.5 µl cDNA, 2.5 µl of 10 µM miRNA specific primer, 2.5 µl miScript Universal Primer, 12.5 µl 2x QuantiTect SYBR Green PCR Master Mix (Qiagen), and 5 µl H_2O, according to the manufacturer's instructions. Cycling parameters were a 15 min 95 °C activation step, followed by 40 cycles of 15s incubation at 94 °C, 30s at a primer specific annealing temperature 55-60 °C, and 30s at 70 °C. After each assay run, specific melting curves were produced by a gradual increase in temperature from 65 °C to 95 °C in 0.5 °C increments every 5s. The final curves were monitored for single peaks to confirm the specificity of the reaction and the absence of primer dimers. Relative transcript abundance derived from standard curves was normalized using the NORMA-Gene approach as described by Heckmann and colleagues (16). Afterwards, miRNA fold changes were calculated relative to the control group and data were analyzed and plotted using Prism Version 7 (Graphpad Software, San Diego, CA, USA). An unpaired t-test was conducted to determine if there were significant differences in specific miRNA expression between groups ($P<0.05$).

3. Results

3.1 Gene expression profiling in PVN of AdrB1.B2 KO chimera mice

There were 477 probes that were differentially expressed in the PVN, which represented 457 unique transcripts ($p<0.05$, FDR corrected) **(Supplemental Data 1 (**https://figshare.com/s/834c2b06aacb6b8162e3, 10.6084/m9.figshare.11495079**)**. Examples of transcripts with decreased abundance in the PVN of the AdrB1.B2 KO chimera mice compared to C57 chimera mice included WAP four-disulfide core domain 17 (Wfdc17, -8.8-fold), Integrin, Alpha X (Complement Component 3 Receptor 4 Subunit) (Itgax, -3.9 fold), and Signal-Regulatory Protein Beta 1 (Sirpb1a, -2.9 fold). Transcripts that were up-regulated in the PVN of the AdrB1.B2 KO chimera mice compared to the control C57 chimera mice included interferon activated gene 202B (Ifi202b, 2.3-fold), Cathepsin E (Ctse, 6.7-fold), and glycerophosphodiester phosphodiesterase domain containing 3 (Gdpd3, 7.1-fold). When clustering data, transcript profiles for each of the two groups did not separate completely by treatment **(Supplemental Figure S1 (**https://figshare.com/s/072e26dcb265d4d48d63, 10.6084/m9.figshare.11495076**).**

Nevertheless, there were a number of transcriptional networks that were differentially expressed in the two groups following bone marrow reconstitution, demonstrating that suppression of the sympathetic drive to the bone alters transcriptional responses in the PVN. Both Tnnt1 (Troponin T1, Slow Skeletal Type) and Prkcd (Protein Kinase C Delta) were confirmed to be decreased in expression based on microarray and real-time PCR **(Supplemental Figure S5 (**https://figshare.com/s/072e26dcb265d4d48d63, 10.6084/m9.figshare.11495076**).**

3.2 Transcriptional networks related to the immune system were suppressed in the PVN of AdrB1.B2 KO chimera mice

Transcripts related to the IS were significantly altered in the PVN of AdrB1.B2 KO chimera mice **(Supplemental Data S2 (**https://figshare.com/s/964aac0cb47e05ccc45e, 10.6084/m9.figshare.11495082**)**. We investigated closely key transcripts that were altered in the PVN, and their relationship to angiotensin (Agt) and the expression levels of Il17, Il17r A and B, tumor necrosis factor receptor (Tnfr), CD4, and NF kappa B1 (Nfkb1) were all decreased as a network **(Figure 1)**. In addition, a gene network related to "activation of microglia" was also decreased in expression in the PVN **(Figure 2)**, along with networks related to macrophage chemotaxis, macrophage function, and macrophage response **(Supplemental Data S2 (**https://figshare.com/s/964aac0cb47e05ccc45e, 10.6084/m9.figshare.11495082**)**. The expression of gene networks related to lymphocytes and T cells were also reduced in relative transcript abundance in the PVN of AdrB1.B2 KO chimera mice compared to controls. Transcripts involved in lymphocyte activation, lymphocyte adhesion, T cell activation, T cell development, T cell recruitment, and T cell tolerance were decreased in the PVN of AdrB1.B2 KO chimera mice **(Supplemental Table 3 (**https://figshare.com/s/072e26dcb265d4d48d63, 10.6084/m9.figshare.11495076**)**. Other cell processes that were differentially expressed included viral transmission, complement activation-alternative pathway, neutrophil activation, mast cell degranulation, and B-cell activation, further suggesting that, in general, there was an overall suppression of transcripts related to the immune system. Despite the majority of immune-related processes being down-regulated, there were some networks that were increased in

median expression and those included immune system responses such as lymphocyte homeostasis, immunocompetence, and immunological surveillance **(Supplemental Table S3 (**https://figshare.com/s/072e26dcb265d4d48d63, 10.6084/m9.figshare.11495076**).**

3.3 Cell processes related to glia and neuronal function were decreased in the PVN of AdrB1.B2 KO chimera mice

Based upon the transcriptomics, glia-related processes decreased and included microglial activation, glial cell development, and glial cell response **(Supplemental Table S3 (**https://figshare.com/s/072e26dcb265d4d48d63, 10.6084/m9.figshare.11495076**).** Transcripts in these pathways included Tgfb1, Cx3cr1, Fgf2, Acxcl10, Ccl2, Csf2, Csf3, CD81, Tnf, and Il6. Neuro-related processes were also suppressed by in the PVN of AdrB1.B2 KO chimera compared to C57 chimera mice, and these processes included dendritic cell differentiation, neuronal activity, neurogenesis, neuron differentiation, and peripheral nerve function among others. Transcripts in these pathways included Gdnf, Ntf3, Igf1, Neurog2, Prl, Runx1, Pomc, among others. Synapse-related processes were also decreased and included long-term synaptic depression, action potential duration transmission of nerve impulse, and generation of action potential. **Figure 3** presents a gene network for glia and neuronal cell processes. All these subnetworks were significantly altered in AdrB1.B2 KO chimera mice **(Supplemental Data 2 (**https://figshare.com/s/964aac0cb47e05ccc45e, 10.6084/m9.figshare.11495082**).**
Lastly, Cell Signaling Pathways, Metabolic Pathways, and Receptor Signaling Pathways were queried for differential expression and it was determined that select neuropeptide signaling pathways were altered in the PVN. For example, VasopressinR1 -> STAT signaling **(Supplemental Figure S2 (**https://figshare.com/s/072e26dcb265d4d48d63, 10.6084/m9.figshare.11495076**)**, Angiopoietin receptor-> FOXO signaling, Oxytocin receptor-> ELK-SRF/GATA/AP-1 signaling, and Neurotensin receptor -> ELK-SRF/AP-1/EGR signaling were all decreased in expression in AdrB1.B2 KO chimera mice relative to controls **(Supplemental Figure S2 (**https://figshare.com/s/072e26dcb265d4d48d63, 10.6084/m9.figshare.11495076**).**

3.4 Diseases associated with changes in the PVN transcriptome in AdrB1.B2 KO chimera mice

There were 214 disease networks affected in the PVN of AdrB1.B2 KO chimera mice **(Supplemental Data 2 (**https://figshare.com/s/964aac0cb47e05ccc45e, 10.6084/m9.figshare.11495082**).** Among these, 169 networks were downregulated in expression in the PVN, and 45 disease networks were upregulated in the PVN of AdrB1.B2 KO chimera mice. Of interest, a disease network related to reactive astrocytosis was significantly downregulated, and included Igf1, Tgfb1, Csf3, Lcn2, and Nf1 genes within the network. Astrocyte function was also downregulated in the PVN, and the associated downregulated transcript included Mmp9, Mmp2, Mapt, Gfap, and Tnf. Other gene-disease networks that were significantly suppressed following bone marrow reconstitution included CNS diseases, brain infarction **(Supplemental Figure S3 (**https://figshare.com/s/072e26dcb265d4d48d63, 10.6084/m9.figshare.11495076**)**, CNS dysfunction, and neuro-inflammation. Moreover, diseases related to immunotoxicity, inflammatory lesions, T helper lymphocyte activity, and T cell infiltration were all downregulated in the PVN of KO chimera. Thus, downregulated gene networks related to diseases of the immune system were particularly prominent in the PVN of AdrB1.B2 KO chimera mice (**Supplemental Data 2 (**https://figshare.com/s/964aac0cb47e05ccc45e, 10.6084/m9.figshare.11495082).

3.5 The expression levels of the renin-angiotensin system-associated transcripts are reduced in the hypothalamus of AdrB1.B2 KO chimera mice

Interestingly, one transcriptional network that was downregulated in the PVN of AdrB1.B2 KO chimera mice was that of the renin-angiotensin system (Ras). Of the 113 known genes associated with this network, based on evidence presented in the literature we captured and measured the relative expression of 105 **(Supplemental Figure S4 (**https://figshare.com/s/072e26dcb265d4d48d63, 10.6084/m9.figshare.11495076**)**. These genes were downregulated, and included genes involved in hormone signaling (Igf1, Agt, VIP, Adrb1, Adrb2, Agtr2, Esr1, Esrrg, and Oxt), Immune activation (Il1b, Il6) and others (Gja5, Tgfb1, Ppara, Epo, Nox1, Mapk8, Nos1).

3.6 miRNA analysis

Based upon the transcriptome analysis, we conducted an *in silico* analysis to identify upstream regulators of the transcriptome. The total number of neighbors are the transcripts regulated by the miR and the number of measured neighbors depicts those measured (Table 1). Perhaps most notable from the *in silico* approach was that many miRNAs were predicted to downregulate their networks. This was also true for many of the miRs measured; miR-150-5p (t=2.40, df=14, p=0.0309), miR-223-3p (t=5.21 df=14, p=0.0001), miR-18a-5p (t=0.8718, df=14, p=0.398), miR-205-5p (t=3.918 df=14, p=0.0015), miR-375-5p (t=2.733, df=14, p=0.0162), miR-499a-5p (t=3.498, df=14, p=0.0036), miR-7b-5p (t=0.3194, df=14, p=0.75), miR-27b-3p (t=3.622 df=14, p=0.0028), let-7a-5p (t=4.010 df=14, p=0.0013), and miR-21a-5p (t=4.82 df=14, p=0.0003). . The sample size was n=8 per group and consisted of the same samples used in the transcriptome analysis.

4. Discussion

Our study uncovers several novel findings: (i) chronic genetic ablation of beta 1 and 2 adrenergic receptors in the BM can alter transcriptional networks in the PVN. This is similar to what has been reported in the gastrointestinal tract of these mice (40); (ii) Neuro-inflammatory networks in the PVN are dampened with reduced sympathetic responsiveness of BM cells; (iii) We identify signaling molecules that contribute to integrated communication between the sympathetic nervous system and BM. Based on our current data, we hypothesize that miRNAs such as miR-150-5p, miR-205-5p and miR-223-3p may be important in mediating transcriptional responses in the PVN; (iv) Non-inverse relationships between miRNA and their predicted targeted mRNA suggest that there may be a temporal component that is needed to more completely characterize the miRNA-mRNA relationships in the PVN following reduced sympathetic responsiveness of the BM. The molecular entities identified in this study nevertheless act as potential therapeutic targets for mitigating the effect of immune system in diseases in which an overactive sympathetic drive is a contributing factor (1, 23, 26, 27).

In our chimera mouse, the effects of the sympathetic drive on the BM have been reduced following a complete reconstitution of the hematopoietic and immune system with BM harvested from a beta 1 and 2 adrenergic receptor KO mice. This results in systemic and tissue-level immunosuppression and reduced blood pressure (4), and a suppression in transcriptional immune networks in the PVN of ArdB1.B2 KO chimera. More specifically, gene networks related to general function and activity of macrophages, lymphocytes, leukocytes, and T cells were reduced in expression. Cell processes that included microglial activation, glial cell development, and glial cell response were also downregulated in the KO chimera, including different inflammatory-related transcripts (e.g. Tgfb1, Cx3cr1, Fgf2, Acxcl10, Ccl2, Csf2, Csf3, CD81, Tnf, and Il6). Downregulation of such immune-related networks in the PVN corresponded with transcriptional suppression of neuronal and synaptic function (e.g. neuronal activity, neurogenesis, neuron differentiation, long-term synaptic depression, action potential duration transmission of nerve impulse, and generation of action potential). This is intriguing; while the hypothalamus was previously considered to be a region of the central nervous system that did not undergo significant neurogenesis, recent studies in the vertebrate adult brain suggest that neuronal differentiation and neurogenesis are essential processes needed to maintaining energy homeostasis and behavior (reviewed in (8)). Indeed, neurons in this region are regulated by a number of sex steroids, neuropeptides and neurogenic signaling molecules. Most interesting is that our previous investigations revealed that neuropeptides are significant factors underlying neurogenic hypertension (43).

The transcriptomic approach in our mouse chimera model identified new pathways that could be associated with dysfunctional sympatho-immune interaction. Here, we report suppression of gene networks associated with diseases such as astrocytosis, CNS diseases, brain infarction, CNS dysfunction, and neuro-inflammation, among others. It appears that transcripts associated with these conditions can be initiated or influenced by changes in systemic immune activity as a function of the effects of the sympathetic nervous system. We also observed downregulation of a number of RAS-related genes in the PVN of KO mouse chimera, suggesting that not only can the central angiotensin II affect the immune system systemically via the sympathetic nervous system (3), but the

systemic immune responses may reciprocally affect the brain RAS at a transcriptome level. . However, it is entirely possible that lowered the blood pressure alone, which we have previously shown to occur in this model (4), could produce the observed changes in gene networks. Further studies are therefore required to elucidate precise mechanisms of the observed transcriptional changes in the brain, but this opens up avenues for novel therapies for CNS conditions associated with immune dysfunction. In addition, studies have revealed connections between neuro-inflammation and neurogenesis in the adult central nervous system (reviewed in (37)). These data suggest that damage to specific brain regions can lead to high activity of pro-inflammatory cytokines (different interleukins) and activation of tumor necrosis factor alpha, further activating microglia, immune cell infiltration, and neurogenesis. The PVN of chimeric mice may also undergo related processes following bone marrow reconstitution. Intriguingly, networks related to neurogenesis and neuro-development were reduced in the PVN which corresponded to suppression of immune-networks, indicating these processes may be correlated in some way in the PVN. Thus, systemic immunosuppression observed here may be linked to suppression of inflammatory networks in the PVN, resulting in altered neuronal activity which underlies over-active sympathetic drive in different diseases (44).

There is little doubt that miRNAs play central roles in the etiology of human diseases that involve chronic inflammatory processes, including cardiovascular disease (39), hypertension (24, 28), obesity (25), and neurodegenerative diseases (20). In the case of miR-150 for example, we measured 122 out of 140 possible downstream targets and this miRNA was down-regulated in the PVN of chimera mice. Studies show that miR-150 can reduce cytokines IL2 and TNF via inhibition of NF-kB signaling (30) under certain conditions, and that it has a significant role in mediating tumorigenesis and inflammation (11, 32). Noteworthy is that we observed a suppression in NF-kB signaling, also involved in regulation of expression of Il-1b, Il17, CCL2 as well as angiotensinogen (AGT) (6, 34, 42). Indeed, it has been reported that anti- TNFα therapy reduced levels of TNFα and Il17, among others, as well as downregulated miR-223-3p in circulation of rheumatoid arthritis patients (7), demonstrating association between miRNAs and clinical and inflammatory parameters. In our model, we also observed downregulation of TNFα, Il17

and miR-223 -3p in the PVN of KO chimera, thus relationships between these molecules may also exist in neuro-immune pathways, and identifies miR-223-3p as a potential therapeutic target in control of aberrant immune responses in the brain. Other differentially expressed miRNAs in the chimera with a role in inflammatory processes included miR-205-5p (17), miR-375-5p in cardiac infarctions (13), and miR-223-3p (33). In fact, miR-223-3p reportedly modulates hematopoietic lineage differentiation and is altered in expression in damaged smooth, skeletal and cardiac muscles, and here we show that it may also be important in regulation of hypothalamic functions in rodents. Thus, many of the miRNAs assessed in this study are regulators in inflammatory processes.

Perhaps most notable from the *in silico* approach was that many miRNAs were predicted to downregulate their transcriptional networks. However, the miRNAs measured here with qPCR were also downregulated, contrary to the expectation of an inverse relationship between miRNAs and their downstream targets. Several explanations may account for this observation. Specific miRNAs in the PVN could be acting in coordination with other factors (e.g. transcription factors) and can form stabilizing or positive correlation loops (9, 41). Thus, we may be capturing an effort in the PVN to stabilize networks in the face of changes rather than one that is driving changing in the system. Alternatively, miRNAs are often involved in negative feedback loops, thus a single snapshot in time may not represent cause and effect as this is time dependent. Additional time points would be required to more accurately assess this possibility. As pointed out by Guo and colleagues (15), these network interactions are complex and difficult to predict. One miRNA can regulate multiple mRNAs and this regulation can be reciprocal. What has become clear over time is that miRNA-mRNA regulatory networks exhibit spatial-temporal patterns of expression that can be somewhat flexible in dynamics.

Neuro-immune communication underscores numerous physiological processes such as blood pressure regulation (3). These data are significant as we identify novel targets for therapeutic interventions for diseases with a neurogenic origin. For example, increased sympathetic drive to the viscera including the BM underlies neurogenic hypertension and there are common molecular targets among studies that may be

beneficial in modifying in order to reduce blood pressure. In a meta-analysis of rodent models, we discovered that transcriptional networks related to kidney function, lactation, neuropeptides (feeding and reproduction), and mitochondrial function were prevalent themes identified as those related to neurogenic hypertension (43). Here, we identify some of the same neuropeptide signaling pathways (e.g. oxytocin and neurotensin), which may act as neuro-immune modulators.

Many diseases have neuro-inflammation as a significant contributor to its etiology and pathology. We identified disease networks and conditions such as astrocyte dysfunction, central nervous system dysfunction, T-helper lymphocyte activity, neutrophil accumulation, and neuroinflammation as suppressed in our chimera mouse; we also revealed a number of novel diseases implicated by the transcriptome response which included Vitamin A Deficiency, Tobacco Use Disorder, and Autistic Disorder to name but a few. Interestingly, a role for vitamin A in neurogenerative diseases (10) and autism (5, 36) have been associated with neuroinflammation. There were fewer disease networks that were up-regulated (e.g. vascular leak syndrome, bone marrow toxicity, Moyamoya Disease, and Acute insulin response). Taken together, the computational analysis underscores the importance of neuroinflammatory processes in the CNS for disease characterization and treatment.

Acknowledgements

This work was supported by 1R56HL136692-01 to JZ and CJM, R21AT010192 Award AWD05242 P0104932 to JZ and CJM, AHA grant 14SDG18300010 to JZ and University of Florida College of Veterinary Medicine (UFCVM) Start Up Funds to JZ and CJM. Funding also through NSERC-DG 147476 to JAM. The authors would like to thank Niousha Ahmari for assistance with RNA isolation, Ty Redler for real-time PCR validation, and Jordan Schmidt for assistance with microarrays.

Figures

Figure 1. A gene network for angiotensin (AGT), IL17, CD4, and NF kappaB which is suppressed in the b1/2-ARs KO chimeras. Blue indicates that relative mRNA levels are decreased for the transcript. The square entities refer to cell processes, the oval entities refer to proteins in general, triangles represent ligands, and receptors are those molecules embedded in the membrane with the mushroom cap. DNA binding factors are those entities indicated with "feet". The arrows indicate direction of entity regulation. Gene identifiers are provided in the abbreviation list **(Supplemental Data 4)**. There was n=8 male mice/group.

Figure 2. An enriched pathway for microglial activation. Red indicates that relative mRNA levels are increased for the transcript, while blue indicates that relative mRNA levels are decreased for the transcript. Shapes and arrows are described in figure caption 1. Gene identifiers are provided in the abbreviation list **(Supplemental Data 4)**. There was n=8 male mice/group.

Figure 3. An enriched transcriptional pathway for cell processes related to neurons and glia. Red indicates that relative mRNA levels are increased for the transcript, while blue indicates that relative mRNA levels are decreased for the transcript. Shapes and arrows are described in figure caption 1. Gene identifiers are provided in the abbreviation list **(Supplemental Data 4)**. There was n=8 male mice/group.

Figure 4. MicroRNA expression in control and KO mice. A) miR150-5p (p=0.031), B) miR-223-3p (p=0.0001), C) miR-18a-5p (p=0.398), D) miR-205-5p (p=0.0015), E) miR-375-5p, p=0.016) miR-499a-5p (p=0.0036), G) miR-7b-5p (p=0.75), H) miR-27b-3p (p=0.0028), I) miR-let-7a-5p (p=0.0013) and J) miR-21a-5p (p=0003). Sample size was n=8 per group.

References

1. **Abboud F, and Kumar R**. Obstructive sleep apnea and insight into mechanisms of sympathetic overactivity. *The Journal of clinical investigation* 124: 1454-1457, 2014.

2. **Abboud FM, Harwani SC, and Chapleau MW**. Autonomic neural regulation of the immune system: implications for hypertension and cardiovascular disease. *Hypertension* 59: 755-762, 2012.

3. **Ahmari N, Santisteban MM, Miller DR, Geis NM, Larkin R, Redler T, Denson H, Khoshbouei H, Baekey DM, and Raizada MK**. Elevated bone marrow sympathetic drive precedes systemic inflammation in angiotensin II hypertension. *American Journal of Physiology-Heart and Circulatory Physiology* 317: H279-H289, 2019.

4. **Ahmari N, Schmidt JT, Krane GA, Malphurs W, Cunningham BE, Owen JL, Martyniuk CJ, and Zubcevic J**. Loss of bone marrow adrenergic beta 1 and 2 receptors modifies transcriptional networks, reduces circulating inflammatory factors, and regulates blood pressure. *Physiological genomics* 48: 526-536, 2016.

5. **Bjørklund G, Saad K, Chirumbolo S, Kern JK, Geier DA, Geier MR, and Urbina MA**. Immune dysfunction and neuroinflammation in autism spectrum disorder. *Acta neurobiologiae experimentalis* 2016.

6. **Brasier AR, Li J, and Copland A**. Transcription factors modulating angiotensinogen gene expression in hepatocytes. *Kidney Int* 46: 1564-1566, 1994.

7. **Castro-Villegas C, Perez-Sanchez C, Escudero A, Filipescu I, Verdu M, Ruiz-Limon P, Aguirre MA, Jimenez-Gomez Y, Font P, Rodriguez-Ariza A, Peinado JR, Collantes-Estevez E, Gonzalez-Conejero R, Martinez C, Barbarroja N, and Lopez-Pedrera C**. Circulating miRNAs as potential biomarkers of therapy effectiveness in rheumatoid arthritis patients treated with anti-TNFalpha. *Arthritis Res Ther* 17: 49, 2015.

8. **Cheng M-F**. Hypothalamic neurogenesis in the adult brain. *Frontiers in neuroendocrinology* 34: 167-178, 2013.

9. **Cora D, Re A, Caselle M, and Bussolino F**. MicroRNA-mediated regulatory circuits: outlook and perspectives. *Phys Biol* 14: 045001, 2017.

10. **Das BC, Dasgupta S, and Ray SK**. Potential therapeutic roles of retinoids for prevention of neuroinflammation and neurodegeneration in Alzheimer's disease. *Neural regeneration research* 14: 1880, 2019.

11. **Davidson-Moncada J, Papavasiliou FN, and Tam W**. MiRNAs of the immune system: roles in inflammation and cancer. *Annals of the New York Academy of Sciences* 1183: 183, 2010.

12. **Ewing G, and Ewing E**. Neuroregulation of the physiological systems by the autonomic nervous system–their relationship to insulin resistance and metabolic syndrome. *Biogenic Amines* 22: 208-239, 2008.

13. **Garikipati VN, Verma SK, Jolardarashi D, Cheng Z, Ibetti J, Cimini M, Tang Y, Khan M, Yue Y, and Benedict C**. Therapeutic inhibition of miR-375 attenuates post-myocardial infarction inflammatory response and left ventricular dysfunction via PDK-1-AKT signalling axis. *Cardiovascular research* 113: 938-949, 2017.

14. **Gaudet AD, Fonken LK, Watkins LR, Nelson RJ, and Popovich PG**. MicroRNAs: roles in regulating neuroinflammation. *The Neuroscientist* 24: 221-245, 2018.

15. **Guo L, Zhao Y, Yang S, Zhang H, and Chen F**. Integrative analysis of miRNA-mRNA and miRNA-miRNA interactions. *BioMed research international* 2014: 2014.

16. **Heckmann L-H, Sørensen PB, Krogh PH, and Sørensen JG**. NORMA-Gene: a simple and robust method for qPCR normalization based on target gene data. *BMC bioinformatics* 12: 250, 2011.

17. **Huo L, Wang Y, Gong Y, Krishnamurthy S, Wang J, Diao L, Liu C-G, Liu X, Lin F, and Symmans WF**. MicroRNA expression profiling identifies decreased expression of miR-205 in inflammatory breast cancer. *Modern Pathology* 29: 330, 2016.

18. **Jun JY, Zubcevic J, Qi Y, Afzal A, Carvajal JM, Thinschmidt JS, Grant MB, Mocco J, and Raizada MK**. Brain-Mediated Dysregulation of the Bone Marrow Activity in Angiotensin II–Induced Hypertension. *Hypertension* 60: 1316-1323, 2012.

19. **Livak KJ, and Schmittgen TD**. Analysis of relative gene expression data using real-time quantitative PCR and the 2(-Delta Delta C(T)) Method. *Methods* 25: 402-408, 2001.

20. **Lukiw W, Dua P, Pogue A, Eicken C, and Hill J**. Upregulation of micro RNA-146a (miRNA-146a), a marker for inflammatory neurodegeneration, in sporadic Creutzfeldt–Jakob disease (sCJD) and Gerstmann–Straussler–Scheinker (GSS) syndrome. *Journal of Toxicology and Environmental Health, Part A* 74: 1460-1468, 2011.

21. **Maestroni GJ**. Adrenergic regulation of haematopoiesis. *Pharmacological research* 32: 249-253, 1995.

22. **Maestroni GJ**. Sympathetic nervous system influence on the innate immune response. *Annals of the New York Academy of Sciences* 1069: 195-207, 2006.

23. **Malpas SC**. Sympathetic nervous system overactivity and its role in the development of cardiovascular disease. *Physiological reviews* 90: 513-557, 2010.

24. **Nemecz M, Alexandru N, Tanko G, and Georgescu A**. Role of microRNA in endothelial dysfunction and hypertension. *Current hypertension reports* 18: 87, 2016.

25. **Ortega FJ, Moreno M, Mercader JM, Moreno-Navarrete JM, Fuentes-Batllevell N, Sabater M, Ricart W, and Fernández-Real JM**. Inflammation triggers specific microRNA profiles in human adipocytes and macrophages and in their supernatants. *Clinical epigenetics* 7: 49, 2015.

26. **Paton JF**. Hypertension–a visceral afferent problem. *Autonomic Neuroscience: Basic and Clinical* 192: 16, 2015.

27. **Paton JF, and Waki H**. Is neurogenic hypertension related to vascular inflammation of the brainstem? *Neuroscience & Biobehavioral Reviews* 33: 89-94, 2009.

28. **Rhodes CJ, Wharton J, Boon RA, Roexe T, Tsang H, Wojciak-Stothard B, Chakrabarti A, Howard LS, Gibbs JSR, and Lawrie A**. Reduced microRNA-150 is associated with poor survival in pulmonary arterial hypertension. *American journal of respiratory and critical care medicine* 187: 294-302, 2013.

29. **Sanders VM, and Kohm AP**. Sympathetic nervous system interaction with the immune system. *International review of neurobiology* 52: 17-41, 2002.

30. **Sang W, Wang Y, Zhang C, Zhang D, Sun C, Niu M, Zhang Z, Wei X, Pan B, and Chen W**. MiR-150 impairs inflammatory cytokine production by targeting ARRB-2 after blocking CD28/B7 costimulatory pathway. *Immunology letters* 172: 1-10, 2016.

31. **Santisteban MM, Ahmari N, Carvajal JM, Zingler MB, Qi Y, Kim S, Joseph J, Garcia-Pereira F, Johnson RD, Shenoy V, Raizada MK, and Zubcevic J**. Involvement of bone marrow cells and neuroinflammation in hypertension. *Circ Res* 117: 178-191, 2015.

32. **Sonkoly E, Ståhle M, and Pivarcsi A**. MicroRNAs and immunity: novel players in the regulation of normal immune function and inflammation. In: *Seminars in cancer biology*Elsevier, 2008, p. 131-140.

33. **Taïbi F, Metzinger-Le Meuth V, Massy ZA, and Metzinger L**. miR-223: an inflammatory oncomiR enters the cardiovascular field. *Biochimica et Biophysica Acta (BBA)-Molecular Basis of Disease* 1842: 1001-1009, 2014.

34. **Thompson WL, and Van Eldik LJ**. Inflammatory cytokines stimulate the chemokines CCL2/MCP-1 and CCL7/MCP-3 through NFkB and MAPK dependent pathways in rat astrocytes [corrected]. *Brain Res* 1287: 47-57, 2009.

35. **Thounaojam MC, Kaushik DK, and Basu A**. MicroRNAs in the brain: it's regulatory role in neuroinflammation. *Molecular neurobiology* 47: 1034-1044, 2013.

36. **Vargas DL, Nascimbene C, Krishnan C, Zimmerman AW, and Pardo CA**. Neuroglial activation and neuroinflammation in the brain of patients with autism. *Annals of Neurology: Official Journal of the American Neurological Association and the Child Neurology Society* 57: 67-81, 2005.

37. **Wang B, and Jin K**. Current perspectives on the link between neuroinflammation and neurogenesis. *Metabolic brain disease* 30: 355-365, 2015.

38. **Wang X, Spandidos A, Wang H, and Seed B**. PrimerBank: a PCR primer database for quantitative gene expression analysis, 2012 update. *Nucleic Acids Res* 40: D1144-1149, 2012.

39. **Wang X, Wang H-X, Li Y-L, Zhang C-C, Zhou C-Y, Wang L, Xia Y-L, Du J, and Li H-H**. MicroRNA Let-7i negatively regulates cardiac inflammation and fibrosis. *Hypertension* 66: 776-785, 2015.

40. **Yang T, Ahmari N, Schmidt JT, Redler T, Arocha R, Pacholec K, Magee KL, Malphurs W, Owen JL, Krane GA, Li E, Wang GP, Vickroy TW, Raizada MK, Martyniuk CJ, and Zubcevic J**. Shifts in the Gut Microbiota Composition Due to Depleted Bone Marrow Beta Adrenergic Signaling Are Associated with Suppressed Inflammatory Transcriptional Networks in the Mouse Colon. *Front Physiol* 8: 220, 2017.

41. **Zhang HM, Kuang S, Xiong X, Gao T, Liu C, and Guo AY**. Transcription factor and microRNA co-regulatory loops: important regulatory motifs in biological processes and diseases. *Brief Bioinform* 16: 45-58, 2015.

42. **Zhou D, Yu T, Chen G, Brown SA, Yu Z, Mattson MP, and Thompson JS**. Effects of NF-kappaB1 (p50) targeted gene disruption on ionizing radiation-induced NF-kappaB activation and TNFalpha, IL-1alpha, IL-1beta and IL-6 mRNA expression in vivo. *Int J Radiat Biol* 77: 763-772, 2001.

43. **Zubcevic J, Baker A, and Martyniuk CJ**. Transcriptional networks in rodent models support a role for gut-brain communication in neurogenic hypertension: a review of the evidence. *Physiological genomics* 49: 327-338, 2017.

44. **Zubcevic J, Waki H, Raizada MK, and Paton JF**. Autonomic-immune-vascular interaction: an emerging concept for neurogenic hypertension. *Hypertension* 57: 1026-1033, 2011.

Table 1: In silico analysis for miR regulators of transcriptome targets measured in the hypothalamus of Adrb1.b2 chimera mice. The total number of neighbors are the transcripts regulated by the miR and the number of measured neighbors depicts those that were measured. Medium fold change and p-value are also provided. Only those miRs showing more than 1.05-fold change are shown in the table but the complete list is provided in Supplemental Data 1.

miRNA	***Total # of Neighbors***	***# of Measured Neighbors***	***Median change***	***p-value***
MIR1276	6	6	-1.21	0.014
m_Mir10a	5	5	-1.20	0.044
MIR466	6	5	-1.13	0.011
MIR885	19	18	-1.12	0.034
MIR507	11	11	-1.10	0.018
m_Mir7b	9	7	-1.09	0.046
MIR27B	174	156	-1.09	0.016
MIR323A	31	27	-1.08	0.027
MIR32	181	171	-1.08	0.025
MIR889	15	11	-1.08	0.040
MIR146B	57	50	-1.07	0.011
MIR194-1	115	101	-1.07	0.025
MIR335	75	60	-1.07	0.047
MIR126	112	101	-1.07	0.003

MIR190A	27	26	-1.07	0.004
MIR383	34	24	-1.06	0.013
MIR330	68	61	-1.06	0.033
MIR320A	109	89	-1.06	0.032
MIR26A1	341	309	-1.06	0.002
MIR223	185	162	-1.06	0.010
MIR18A	121	111	-1.06	0.044
MIR515-1	12	9	-1.06	0.017
MIR222	160	135	-1.06	0.016
MIR144	289	256	-1.05	0.009
MIR326	44	40	-1.05	0.013
MIR205	156	138	-1.05	0.023
MIR150	140	122	-1.05	0.030
m_Mir743b	11	9	-1.05	0.043
MIR708	28	26	1.05	0.040

638

639

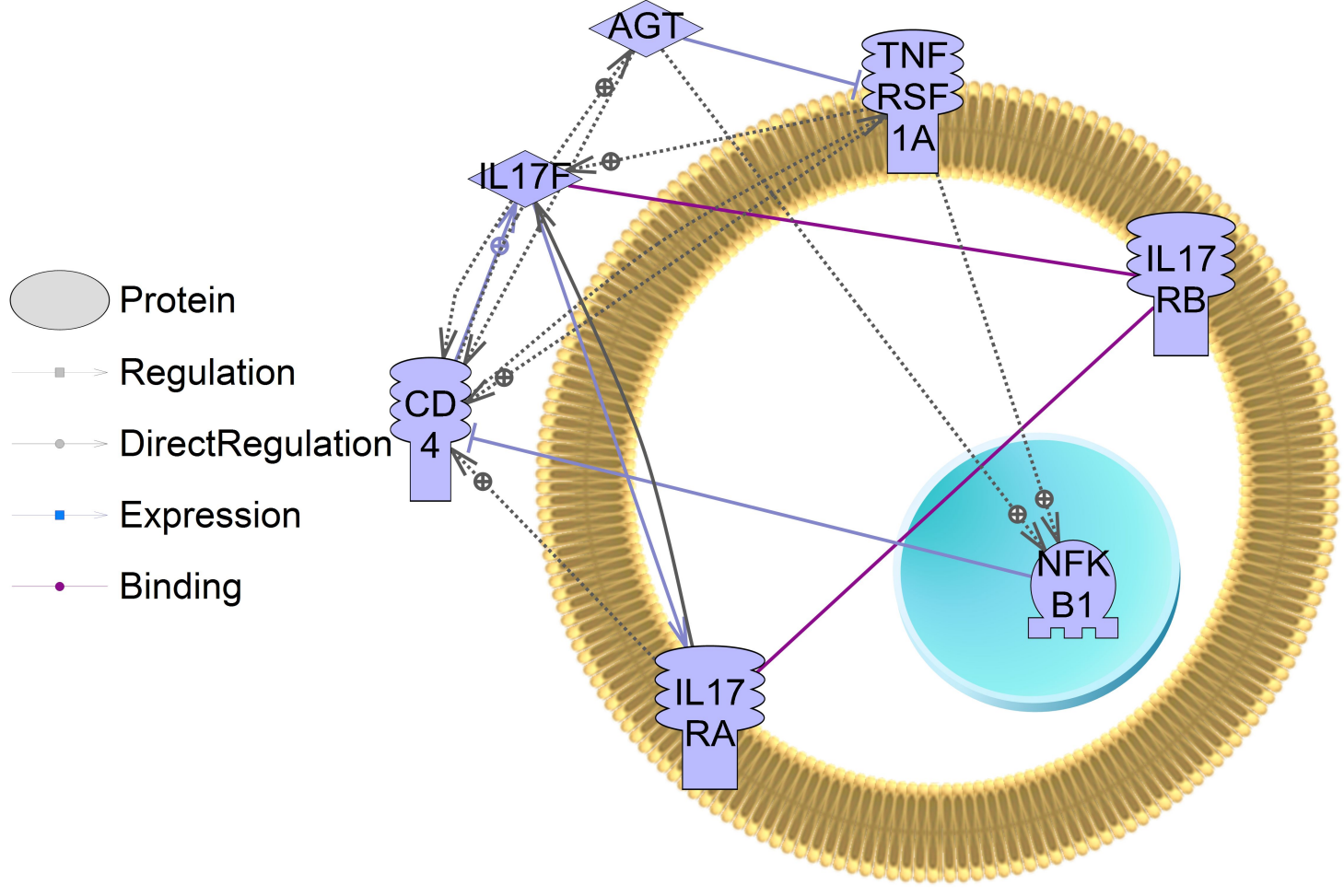
AGT
TNF
RSF
1A
IL17F
IL17
RB
CD
4
NFK
B1
IL17
RA
Protein
Regulation
DirectRegulation
Expression
Binding

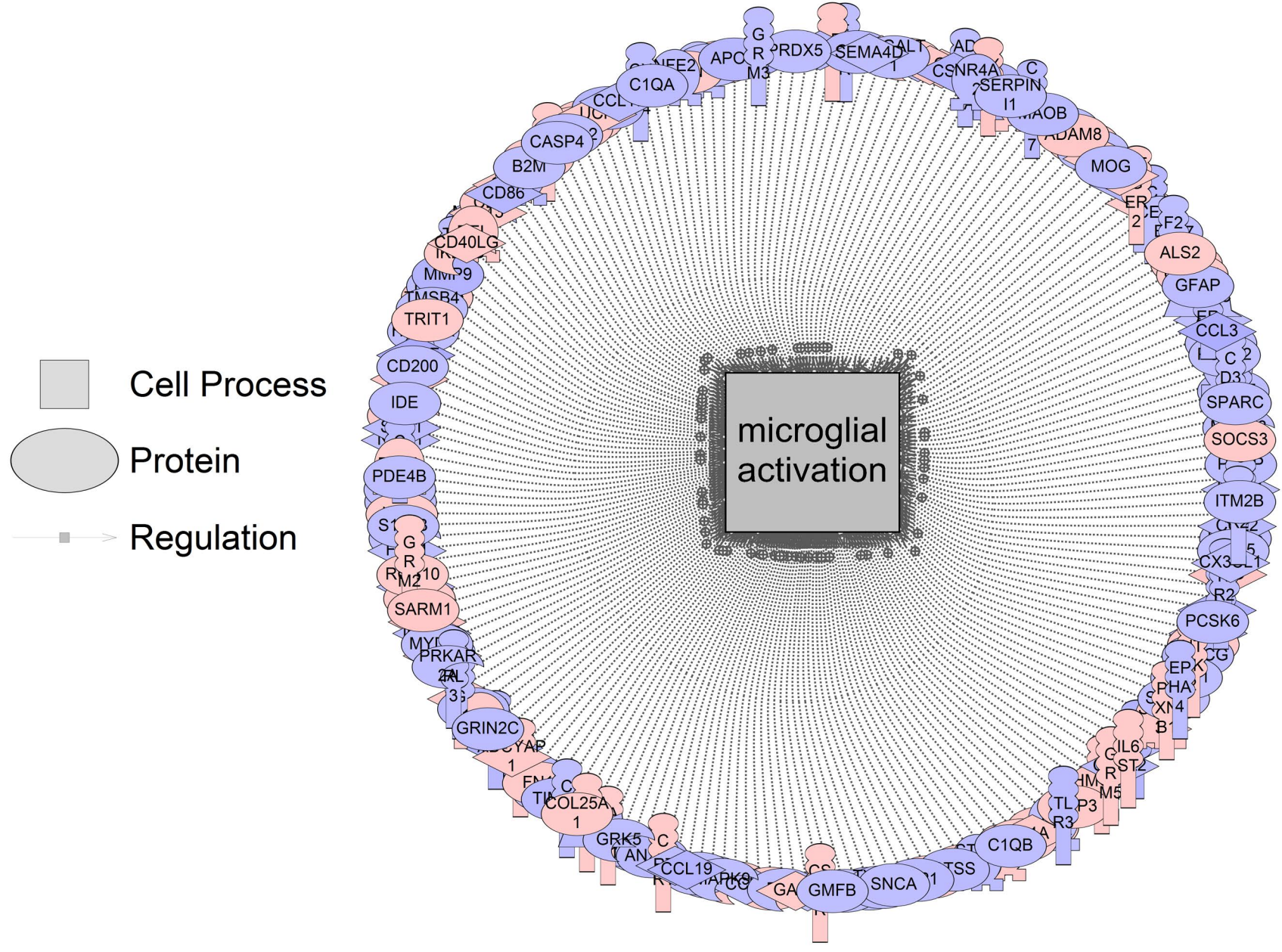
Cell Process
Protein
Regulation
microglial activation
C1QA
CASP4
B2M
CD86
CD40LG
TRIT1
CD200
IDE
PDE4B
SARM1
GRIN2C
COL25A1
GRK5
CCL19
GMFB
SNCA
C1QB
PCSK6
ITM2B
SOCS3
SPARC
CCL3
GFAP
ALS2
MOG
ADAM8
SERPINI1
SEMA4D
PRDX5

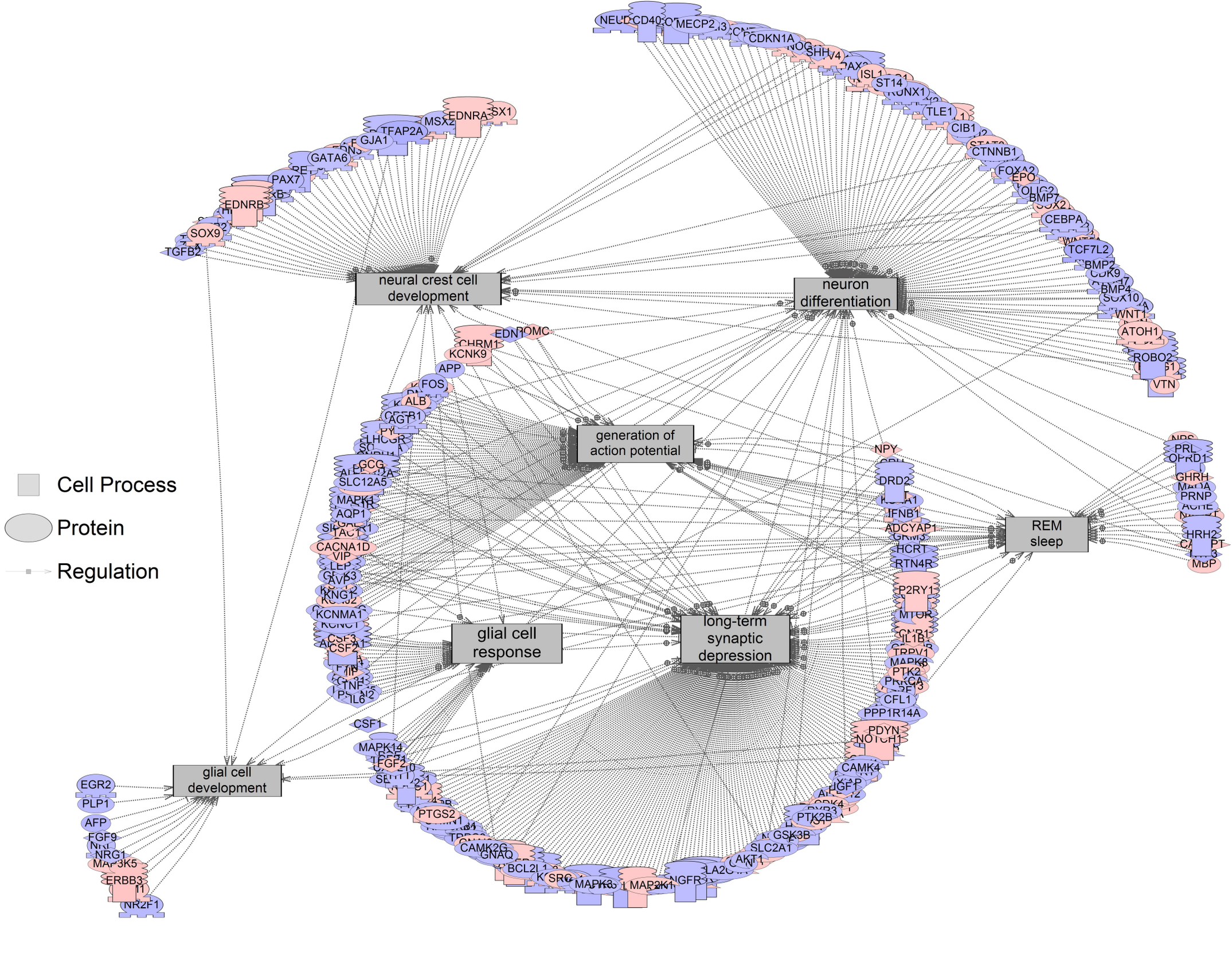
Cell Process
Protein
Regulation
neural crest cell development
neuron differentiation
generation of action potential
REM sleep
glial cell response
long-term synaptic depression
glial cell development
EDNRA
MSX1
TFAP2A
GJA1
GATA6
PAX7
EDNRB
SOX9
TGFB2
CDKN1A
SHH
ISL1
ST14
RUNX1
TLE1
CIB1
CTNNB1
FOXA2
EPO
BMP7
SOX2
CEBPA
TCF7L2
BMP2
CDK9
BMP4
SOX10
WNT1
ATOH1
ROBO2
VTN
EDN1
CHRM1
KCNK9
APP
FOS
ALB
AGT
LHCGR
GCG
SLC12A5
MAPK8
AQP1
TAC1
CACNA1D
VIP
LEP
AVP
KCNA2
KCNMA1
CSF3
CSF2
TNF
IL6
NPY
DRD2
IFNB1
ADCYAP1
HCRT
RTN4R
PRL
OPRD1
GHRH
PRNP
HRH2
MBP
P2RY1
MTOR
IL1B
TRPV1
MAPK8
PTK2
CFL1
PPP1R14A
PDYN
NOTCH1
CAMK4
PTK2B
GSK3B
SLC2A1
AKT1
NGFR
MAPK3
MAP2K1
SRC
BCL2L1
GNAQ
CAMK2G
CSF1
MAPK14
FGF2
PTGS2
EGR2
PLP1
AFP
FGF9
NRG1
MAP3K5
ERBB3
NR2F1

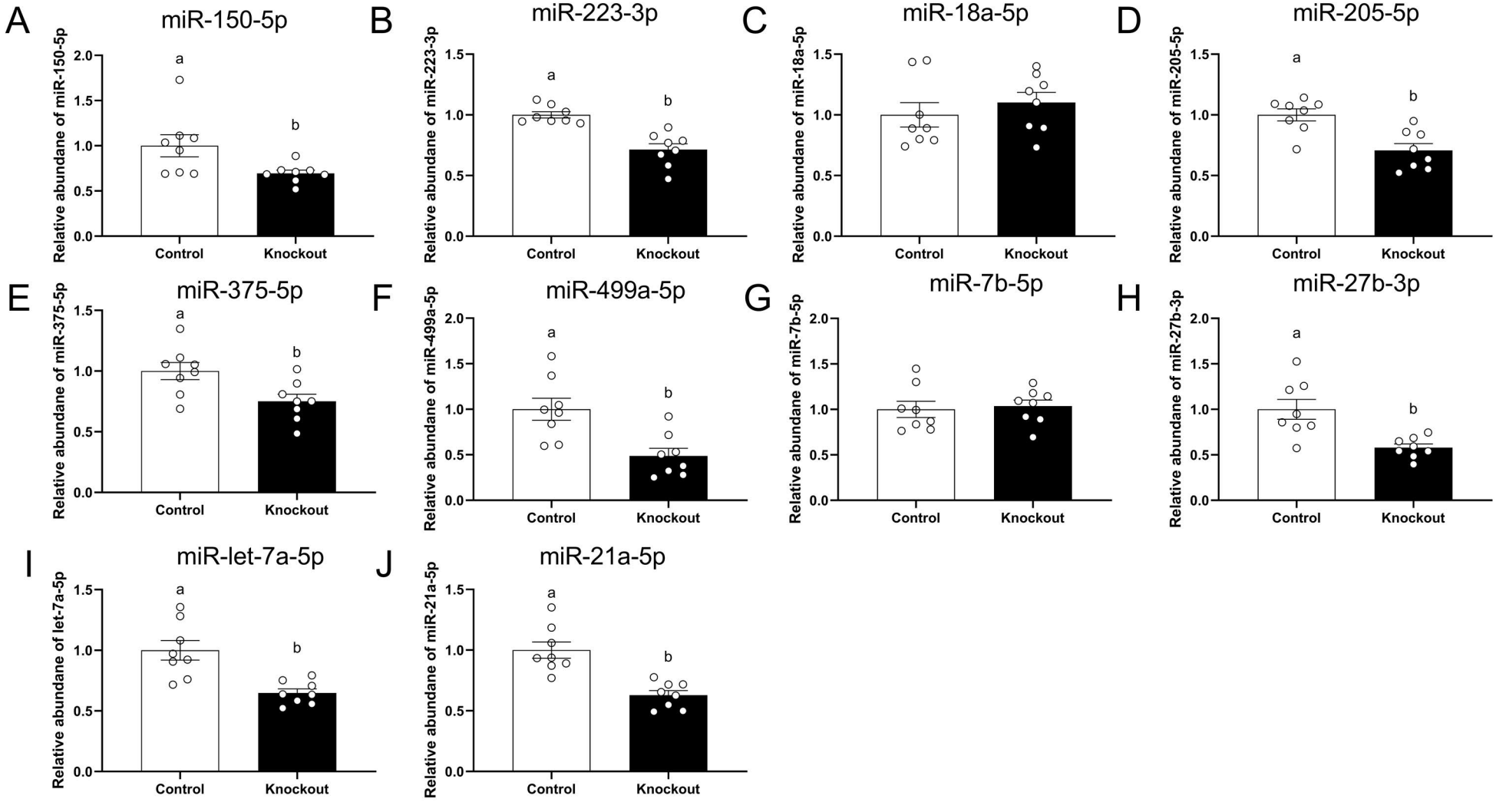
A
miR-150-5p
Relative abundane of miR-150-5p
B
miR-223-3p
Relative abundane of miR-223-3p
C
miR-18a-5p
Relative abundane of miR-18a-5p
D
miR-205-5p
Relative abundane of miR-205-5p
E
miR-375-5p
Relative abundane of miR-375-5p
F
miR-499a-5p
Relative abundane of miR-499a-5p
G
miR-7b-5p
Relative abundane of miR-7b-5p
H
miR-27b-3p
Relative abundane of miR-27b-3p
I
miR-let-7a-5p
Relative abundane of let-7a-5p
J
miR-21a-5p
Relative abundane of miR-21a-5p
Control
Knockout
a
b